The Accuracy of Finite-Difference Solutions of Laplace's Equation

JAMES W. DUNCAN, SENIOR MEMBER

Abstract—**The cross sections of most TEM mode transmission lines have reentrant corners or edges where the potential gradient is singular. In this paper the accuracy of the finite-difference solution for the electric field normal to the conductor boundary at a right-angle corner and at the edge of a thin plate is examined. The accuracy of the finite-difference solution is related to the mesh length h, the magnitude of the lattice point residuals, and the finite-difference operator which is used in place of the Laplacian differential operator. The computing time required to solve the mesh equations by the method of successive overrelaxation is specified. The surface charge density in the neighborhood of the boundary singularity is expressed as a truncated series of circular harmonics. As a result, the integral of the surface charge can be calculated with very good accuracy. The paper concludes by using the harmonic series treatment to determine the capacitance per unit length of a square coaxial transmission line.**

I. Introduction

THE CHARACTERISTIC impedance and attenuation constant of TEM mode transmission lines can be determined with considerable facility by the method of finite differences. Green[1] and Schneider[2] have published solutions obtained by the finite-difference technique for some particularly difficult stripline configurations. The author has used this method to determine the even and odd mode impedances of offset parallel-coupled strip transmission lines. These data were used in the design of a tapered-line hybrid junction which operates over a frequency bandwidth of 0.7 to 12.5 GHz.[3] Getsinger[4] and Shelton[5] have published approximate solutions for infinitely thin conductors in the offset configuration which were obtained by the mapping approximation method. Recently, Carson and Cambrell[6] used a variational formula (field energy integral) in conjunction with the finite-difference method to calculate characteristic impedance.

When one treats a potential problem by the finite-difference method he is immediately faced with the perplexing task of estimating the accuracy of the numerical solution. For most problems of interest, there is no theoretical error bound available because practical transmission lines usually have boundaries with sharp edges or reentrant corners where the potential gradient is singular. All estimates of the mesh or "discretization error" depend on the continuity of higher-order partial derivatives and these estimates fail when the gradient is singular on the boundary.[7] The finite-difference solution is inaccurate near the field singularity and the error spreads to neighboring mesh points. As a result, special treatment is required to obtain accurate results near reentrant corners. This is particularly important, for example, when calculating the attenuation constant of the line where one must integrate the normal electric field over the conductor boundaries.

In this paper we have investigated the accuracy of the finite-difference solution for the potential gradient along the conductor boundary near a reentrant corner. For this purpose we have selected the infinite right-angle bend and the semi-infinite plate between parallel ground planes because each configuration may be solved exactly by means of conformal mapping. Thus the finite-difference solution and the exact solution may be compared to determine the error distribution near the field singularity. Moreover, the accuracy of the finite-difference solution may be exhibited as it relates to the mesh length h, the absolute magnitude of the lattice point residuals, and the finite-difference formulas which are used in place of the Laplacian operator.

In order to improve the numerical solution in the vicinity of reentrant corners we have followed Motz's earlier work[9] and written a harmonic series expansion for the field in the neighborhood of the singularity. The series expansion yields the correct singular behavior of the field at the boundary corner. The series coefficients are specified by equating the series expansion to the potential gradient at selected points on the boundary. Thus the normal electric field (or surface charge density) is accurately determined in the entire neighborhood of the corner and the integral of the charge density can be calculated to an accuracy of a fraction of a percent. The paper concludes by using the harmonic series treatment to arrive at the capacitance per unit length of a square coaxial transmission line. The results are compared to the exact solution available from conformal mapping.

II. The Finite-Difference Method

The electrical parameters of the TEM mode transmission line follow from the solution of Laplace's equation

$$\Delta\phi = \frac{\partial^2\phi}{\partial x^2} + \frac{\partial^2\phi}{\partial y^2} = 0 \tag{1}$$

over the two dimensional domain comprising the transverse cross section of the line.[10] The approximate solution of Laplace's equation by the finite-difference method is effected by superposing a square lattice or mesh over the region and solving the system of equations for the potential $\phi(x_j, y_k)$ at the discrete nodes which are the intersection points of the lattice. In Fig. 1 we show a portion of the square mesh using a simple subscript notation to identify the lattice points of

Manuscript received February 16, 1967.

The author is with the Ground Systems Group, Hughes Aircraft Company, Fullerton, Calif.

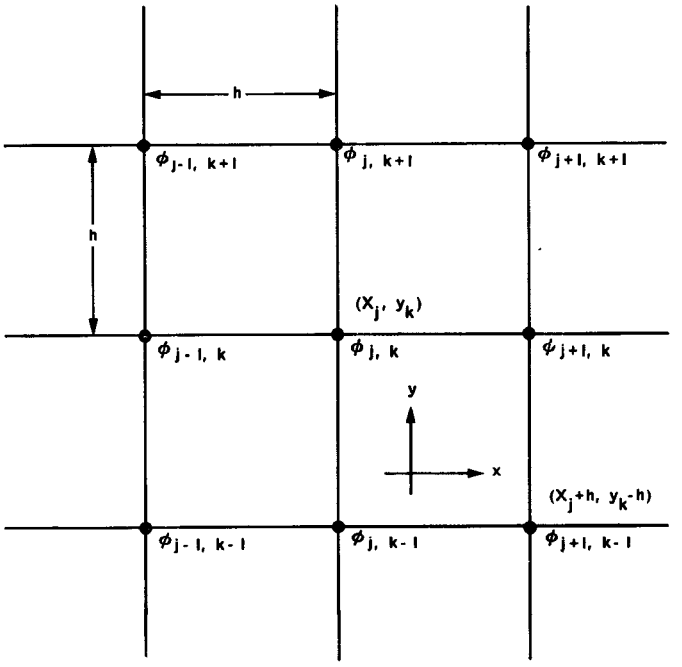

Fig. 1. Finite-difference lattice.

the subregion. The coordinates (x_j, y_k) of a lattice point are defined by

$$x_j = x_0 + jh,$$
$$y_k = y_0 + kh, \qquad j, k = 0, \pm 1, \pm 2, \cdots, \tag{2}$$

where (x_0, y_0) is an arbitrary origin for the "mesh coordinates" (j, k) and h is the mesh length between adjacent lattice points. By definition $\phi_{j,k}$ is the potential at node (x_j, y_k) and, for example, $\phi_{j+1,k-1}$ is the potential at the node (x_j+h, y_k-h).

The five-point Laplace difference operator is defined

$$\Delta^{(5)}\phi = \frac{1}{h^2}\left[\phi_{j-1,k} + \phi_{j,k+1} + \phi_{j,k-1} + \phi_{j+1,k} - 4\phi_{j,k}\right]. \tag{3}$$

The nine-point operator, which includes the potentials at the four diagonal lattice points, is defined

$$\Delta^{(9)}\phi = \frac{1}{6h^2}\left[4(\phi_{j-1,k} + \phi_{j,k+1} + \phi_{j+1,k} + \phi_{j,k-1}) + (\phi_{j-1,k-1} + \phi_{j+1,k+1} + \phi_{j-1,k+1} + \phi_{j+1,k-1}) - 20\phi_{j,k}\right]. \tag{4}$$

Expressing the node potentials in infinite series using Taylor's formula, Kantorovich and Krylov[11] derive the following expansions for the five- and nine-point operators:

$$\Delta^{(5)}\phi = \Delta\phi + \frac{2h^2}{4!}\left(\frac{\partial^4\phi}{\partial x^4} + \frac{\partial^4\phi}{\partial y^4}\right) + \cdots \tag{5}$$

and

$$\Delta^{(9)}\phi = \Delta\phi + \frac{40}{3}\frac{h^6}{8!}\left(\frac{\partial^8\phi}{\partial x^4 \partial y^4}\right) + \cdots. \tag{6}$$

Because ϕ is harmonic and satisfies $\Delta\phi = 0$, (5) indicates that the error committed in writing $\Delta^{(5)}\phi = 0$ to determine $\phi_{j,k}$ is of order h^2 as h tends to zero. Correspondingly, (6) indicates an error of order h^6 in $\Delta^{(9)}\phi = 0$. However, both (5) and (6) assume the continuity of higher-order partial derivatives of ϕ over the square region $[x_j-h, x_j+h]$, $[y_k-h, y_k+h]$. Because the potential gradient is singular at a reentrant corner, (5) and (6) are not applicable at the nodes immediately adjacent to the corner and it is not apparent which operator would yield the more accurate results. As noted, the effect of the boundary singularity spreads to neighboring mesh points and, in terms of h, the order of magnitude of the discretization error is unknown. To quote from Forsythe and Wasow,[8] "There is some numerical evidence that re-entrant angles may actually modify the order of magnitude of the discretization error globally." This view is substantiated in results presented in Section III, where it is shown that the five-point formula yielded solutions more accurate than the nine-point formula when calculating the potential gradient about a 90 degree corner.

The formula for computing the potential $\phi_{j,k}$ using the approximation $\Delta^{(5)}\phi = 0$ follows from (3):

$$\phi_{j,k} = \tfrac{1}{4}\left[\phi_{j-1,k} + \phi_{j,k+1} + \phi_{j,k-1} + \phi_{j+1,k}\right]. \tag{7}$$

The system of equations generated by (7) was solved by the Young-Frankel method of successive overrelaxation.[12],[13] The acceleration parameter ω which appears in the successive overrelaxation formula was determined in the course of iteration as proposed by Carré.[14] The potential at each lattice point was computed in sequence by advancing from the bottom to the top of the mesh in each column of nodes and from left to right in successive columns. A complete scanning of the region constitutes one iteration cycle. Let the superscript (n) denote the current iteration cycle and, therefore, $(n-1)$ denotes the previous cycle. As a result of the lattice point scanning sequence, the successive overrelaxation formula for $\Delta^{(5)}\phi$ reads

$$\phi_{j,k}^{(n)} = (1-\omega)\phi_{j,k}^{(n-1)} + \frac{\omega}{4}\left[\phi_{j-1,k}^{(n)} + \phi_{j,k+1}^{(n-1)} + \phi_{j,k-1}^{(n)} + \phi_{j+1,k}^{(n-1)}\right]. \tag{8}$$

For the five-point operator, the residual $\delta_{j,k}$ at an interior node (x_j, y_k) is defined

$$\delta_{j,k} = (\phi_{j-1,k} + \phi_{j,k+1} + \phi_{j,k-1} + \phi_{j+1,k} - 4\phi_{j,k}). \tag{9}$$

The iterative process was terminated by requiring that all node residuals satisfy

$$|\delta_{j,k}| < m \tag{10}$$

where the positive constant $m=10^{-p}$, with p in the range $2\leq p\leq 6$. The maximum boundary potential for the regions was unity. Thus, the residuals were reduced to a magnitude of from 1.0 to 0.0001 percent of the maximum boundary potential. Expressions similar to (7), (8), and (9) for the operator $\Delta^{(9)}\phi$ follow from (4).

The mesh error, which is a function of the mesh length h, occurs because the finite-difference operator is used in place of the Laplacian. In addition to the mesh error, the finite-difference solution is subject to "iteration error" because the system of linear equations is not solved exactly by the iterative process. Let ρ be the radius of a circle with center at node (x_0, y_0) which just encloses the region of the mesh problem. Milne[15] shows that if the maximum residual $|\delta_{j,k}|_{\max}$ does not exceed a positive quantity m, the maximum error in the iterative solution does not exceed $m\rho^2/4h^2$ for the five-point operator and $m\rho^2/24h^2$ for the nine-point operator. These results indicate that as one uses a finer mesh (larger ρ/h) in order to reduce the mesh error, the maximum residual m must be decreased proportionately (leading to more iteration cycles) in order to satisfy the same iteration error bound.

III. Comparison of Solutions

With the preceding discussion of the error problem in mind, we shall compare the numerical finite-difference solution and the exact solution obtained from conformal mapping for the two geometrical cross sections shown in Fig. 2. The characteristic dimensions of the infinite right-angle bend and the semi-infinite plate between conducting planes, as well as the boundary conditions on the potential ϕ, are given in the figure. The exact solution of Laplace's equation for each boundary value problem is obtained by applying the Schwarz-Christoffel transformation to the respective z-plane polygon.[16]

We shall examine the electric field intensity $|\partial\phi/\partial n|$ normal to the conducting boundary $Q'C'P'$ of the right-angle bend. The field intensity is singular at the 90 degree re-entrant corner which is vertex C'. In order to carry out the finite-difference method, the potential must be specified at all nodes on the boundary surrounding the region. Thus $\phi=0$ at nodes along QCP and $\phi=1$ at nodes along $Q'C'P'$. A linear potential distribution progressing from zero to unity was specified for the nodes along boundaries PP' and QQ'. As a result, the potential gradient at vertices P' and Q' has the value $1/b$ and $1/g$, respectively. If we then specify the side lengths CP and CQ by the relations

$$CP = g + 2.7b,$$
$$CQ = b + 2.7g \tag{11}$$

it results that the potential gradient at the locations P' and Q' is in error by less than 0.01 percent of the exact solution.

In the case of the semi-infinite plate between parallel planes, we shall examine the potential gradient normal to the boundary surface CD. Because of the symmetry of the cross section, the finite-difference procedure may be applied to only one-half of the figure, the polygon $ABCDEF$, for example. A linear potential distribution was prescribed for nodes along boundary BC with the length $CD=2.7$ $BC=2.7(d-t)/2$. The potentials at nodes along EF were determined in the course of iteration under the condition that EF is a magnetic wall or plane of symmetry of the potential field. The potentials at nodes along AF were set equal to zero. By specifying the length $EF=2.8d$, it follows from the conformal mapping solution that the error in the node potentials along AF is not greater than 0.01 percent.

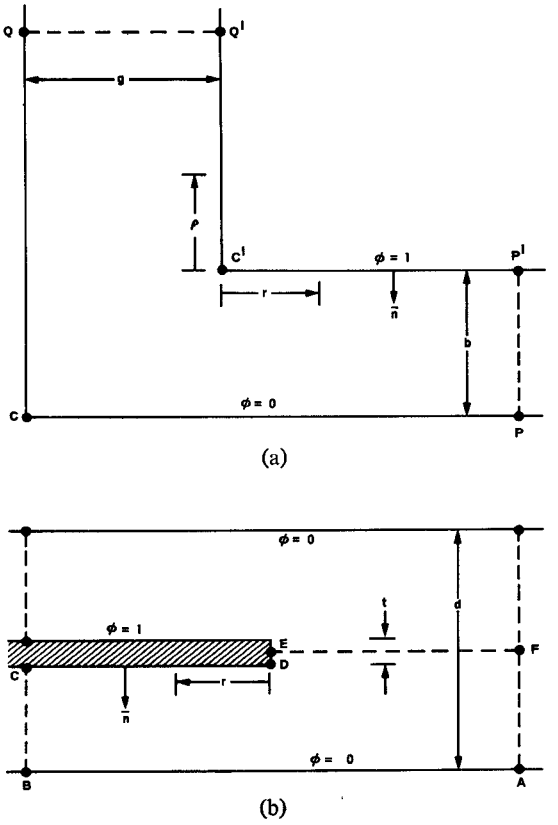

Fig. 2. (a) Infinite right-angle bend. (b) Semi-infinite plate between parallel planes.

The potential gradient normal to the boundary surface was calculated using a five-point formula given by Bickley,[17]

$$\left|\frac{\partial\phi}{\partial n}\right| = \frac{1}{24h}\left[50\phi_0 - 96\phi_1 + 72\phi_2 - 32\phi_3 + 6\phi_4\right] \tag{12}$$

where $\phi_0, \phi_1, \cdots, \phi_4$ are the potentials at successive nodes in the direction normal to the boundary with ϕ_0 designating the boundary potential. The error in this formula is of order h^5, where the mesh length h is the tabular interval.

The right-angle bend was solved by successive overrelaxation using the five-point and nine-point difference operators. Typical results are given in Fig. 3 which shows the percent error in the potential gradient normal to the boundary $Q'C'P'$ for an asymmetrical bend where $g=2b$ and $b/h=16$.

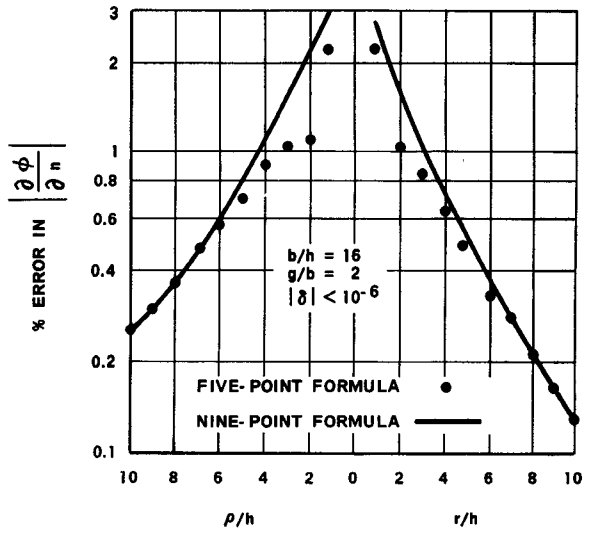

Fig. 3. Percent error in $|\partial\phi/\partial n|$ about a 90 degree corner ($g=2b$).

The abscissa is distance measured from the corner in terms of the mesh length h. The surprising result evident in Fig. 3 was substantiated in all calculations of the right-angle bend, that is, that the five-point operator yielded the more accurate solutions. When the semi-infinite plate was treated, the two operators were not compared, only the five-point operator was used. Fig. 3 also serves to demonstrate the increasing error in the finite-difference solution as the corner singularity is approached ($r, \rho \rightarrow 0$).

We are interested in the accuracy that can be realized for a given amount of computing time. The machine time required by the finite-difference method is directly proportional to the number of interior nodes which are scanned per iteration cycle and, of course, the number of cycles that are necessary to satisfy the residual criterion. The number of interior nodes is a function of the mesh division. When the mesh length is halved in order to reduce the mesh error, the number of interior nodes increases by more than a factor of 4, and the computing time increases proportionately. Moreover, when the mesh is made finer, more iteration cycles are necessary to satisfy the *same* residual criterion. In the tables which follow, we shall examine the accuracy of the finite-difference solution and the resultant computing time as they are determined by the mesh size and the residual test constant $m=10^{-p}$. All calculations were carried out using the five-point operator.

In Table I we show the percent error in $|\partial\phi/\partial n|$ as a function of the mesh size for the symmetrical right-angle bend ($g=b$). The potential gradient is calculated at selected positions r/b along the boundary $C'P'$. The residual test constant $m=10^{-6}$. The column $b/h=\infty$ corresponds to an estimate of the solution for zero mesh length and was obtained using Richardson's method of extrapolation[18] in which we assume that the mesh error is proportional to h^2. Obviously, this procedure is questionable for problems with reentrant corners. The extrapolated solution, which was calculated from the $b/h=16$ and $b/h=32$ solutions, was found to be only slightly improved over the $b/h=32$ result.

The machine times required to effect solutions for various mesh divisions are given in Table II, which shows the number of interior nodes for a given b/h and the number of iteration cycles necessary to satisfy the residual test $|\delta_{j,k}| < 10^{-4}$. Notice that the computing times of Table II do not apply to the results shown in Table I which were obtained under the condition $m=10^{-6}$. The times shown include all of the calculations which were required to compare the numerical and the exact solutions. The computer was an IBM 7094. Notice how the number of iteration cycles increases as the mesh is made finer in order to satisfy the same residual criterion $m=10^{-4}$.

The effect of m on the finite-difference solution is indicated in Table III which shows the percent error in $|\partial\phi/\partial n|$ at various positions r/b for three values of m. These data are for the mesh division $b/h=32$ which yields 6355 interior nodes. Notice that the normal gradients are more accurate when $m=10^{-4}$ than when $m=10^{-6}$, although the error decreases monotonically with increasing r only for the case $m=10^{-6}$. When the coarse mesh $b/h=8$ with 357 interior nodes was used, the solutions for $m=10^{-4}$ and 10^{-6} were identical. The case $m=10^{-2}$ was not calculated but presumably it was the same.

The computing time varies substantially with m when a relatively fine mesh is used. Table IV shows computing time as a function of m for the mesh division $b/h=32$. Notice that the time is doubled by decreasing m from 10^{-4} to 10^{-6} although Table III shows that $m=10^{-4}$ yielded the more accurate results. When the coarse mesh $b/h=8$ was used, the number of iteration cycles was essentially the same for $m=10^{-4}$ and $m=10^{-6}$, consequently, the machine time was identical.

In Tables V through VIII, we present information similar to the foregoing but the data pertain to the semi-infinite plate between parallel planes. In all cases the plate thickness $t=d/10$. Table V shows the percent error in $|\partial\phi/\partial n|$ at selected positions r/d along the boundary CD. The residual test constant $m=10^{-6}$. The column $d/h=\infty$ corresponds to the extrapolated solution (assuming mesh error of order h^2) obtained from the $d/h=20$ and $d/h=40$ solutions. As may be seen, the extrapolated solution is only slightly more accurate than the $d/h=40$ solution.

The number of iteration cycles and the machine time necessary to obtain the solutions of Table V are shown in Table VI. Notice that the computing time increases by a factor of 13 when the mesh division changes from $d/h=40$ to $d/h=100$. However, as Table V shows, the reduction in mesh error effected with $d/h=100$ is not commensurate with the inordinate increase in machine time.

Table VII shows the effect of m, on the accuracy of the solution for the mesh division $d/h=100$ which yields 19 318 interior nodes. The distribution of error with m is quite similar to the data of Table III which applies to the right-angle bend with 6355 interior nodes. Notice that $m=10^{-4}$

TABLE I

PERCENT ERROR IN $|\partial\phi/\partial n|$ RIGHT-ANGLE BEND $g=b$ $m=10^{-6}$

r/b \ b/h	8	16	32	∞
0.125	1.88	1.00	0.832	0.775
0.250	0.689	0.695	0.344	0.228
0.375	0.570	0.394	0.174	0.100
0.500	0.410	0.227	0.098	0.055
0.750	0.169	0.084	0.036	0.021
1.000	0.063	0.032	0.014	0.0076

TABLE II

NUMBER OF ITERATION CYCLES AND COMPUTING TIME, RIGHT-ANGLE BEND, $g=b$, $m=10^{-4}$

b/h	Interior Nodes	Iteration Cycles	Time (s)
8	357	49	5
16	1545	73	25
20	2413	85	43
32	6355	109	48

TABLE III

PERCENT ERROR IN $|\partial\phi/\partial n|$, RIGHT-ANGLE BEND, $g=b$, $b/h=32$

r/b \ m	10^{-2}	10^{-4}	10^{-6}
0.0625	0.406	0.871	1.131
0.125	0.139	0.593	0.832
0.1875	0.139	0.308	0.523
0.250	0.285	0.152	0.344
0.3125	0.354	0.072	0.240
0.375	0.380	0.030	0.174
0.4375	0.379	0.008	0.129
0.500	0.361	0.004	0.098
0.5625	0.332	0.010	0.076
0.625	0.295	0.011	0.059
0.6875	0.256	0.011	0.046
0.750	0.219	0.013	0.036

TABLE IV

NUMBER OF ITERATION CYCLES AND COMPUTING TIME, RIGHT ANGLE BEND, $g=b$, $b/h=32$

m	Interior Nodes	Iteration Cycles	Time (s)
10^{-2}	6355	97	44
10^{-4}	6355	109	48
10^{-6}	6355	169	96

TABLE V

PERCENT ERROR IN $|\partial\phi/\partial n|$, SEMI-INFINITE PLATE, $t=d/10$, $m=10^{-6}$

r/d \ d/h	20	40	100	∞
0.05	2.506	1.241	0.778	0.819
0.10	1.088	0.879	0.317	0.809
0.15	0.866	0.522	0.167	0.408
0.20	0.629	0.318	0.099	0.214
0.25	0.431	0.202	0.062	0.125
0.30	0.289	0.131	0.040	0.079
0.35	0.192	0.087	0.025	0.052
0.40	0.128	0.058	0.016	0.035

TABLE VI

NUMBER OF ITERATION CYCLES AND COMPUTING TIME, SEMI-INFINITE PLATE, $t=d/10$, $m=10^{-6}$

d/h	Interior Nodes	Iteration Cycles	Time (s)
20	750	97	7
40	3053	217	53
100	19 318	493	702

TABLE VII

PERCENT ERROR IN $|\partial\phi/\partial n|$, SEMI-INFINITE PLATE, $t=d/10$, $d/h=100$

r/d \ m	10^{-2}	10^{-4}	10^{-6}
0.02	5.43	0.688	1.25
0.04	5.10	0.463	0.960
0.06	4.94	0.184	0.631
0.08	4.72	0.031	0.435
0.10	4.46	0.048	0.317
0.12	4.19	0.089	0.241
0.14	3.94	0.112	0.188
0.16	3.70	0.123	0.150
0.18	3.47	0.126	0.122
0.20	3.26	0.126	0.099
0.30	2.39	0.100	0.040
0.40	1.81	0.072	0.016

TABLE VIII

NUMBER OF ITERATION CYCLES AND COMPUTING TIME, SEMI-INFINITE PLATE, $t=d/10$, $d/h=100$

m	Interior Nodes	Iteration Cycles	Time (min)
10^{-2}	19 318	97	3.10
10^{-4}	19 318	205	5.45
10^{-6}	19 318	493	11.7

TABLE IX

PERCENT ERROR IN $|\partial\phi/\partial n|$, SEMI-INFINITE PLATE, $d/h=100$, $m=10^{-6}$

r/h \ t/d	0.02	0.04	0.10
1	2.91	2.65	2.42
2	1.76	1.46	1.25
3	1.62	1.35	1.14
4	1.39	1.15	0.96
5	1.15	0.95	0.78
6	0.95	0.78	0.63
7	0.80	0.65	0.52
8	0.68	0.55	0.43
9	0.59	0.47	0.37
10	0.51	0.41	0.32

yields the more accurate results until r measures 18 mesh lengths from the plate edge ($r/d=0.18$), thereafter, the solutions for $m=10^{-6}$ are more accurate but the difference is not particularly significant. The difference in computing time between the cases $m=10^{-4}$ and $m=10^{-6}$ is, however, very significant as is evident in Table VIII. Obviously, $m=10^{-2}$ is not an adequate residual requirement for a mesh division which yields thousands of lattice points. In contrast to Table VII, when the coarse mesh $d/h=20$ was used to solve the semi-infinite plate problem, the solutions for $m=10^{-2}$, 10^{-4}, and 10^{-6} were almost identical over the entire range of r which was investigated ($0\leq r/d\leq 0.5$). The computing time was about 7 seconds for each value of m when $d/h=20$. Lastly, in Table IX, we show the error distribution that results for the semi-infinite plate when the plate thickness $t/d=0.02$, 0.04, and 0.10. Table IX may be compared to Fig. 3 to see the more pronounced effect that the "edge singularity" has in propagating errors in the neighborhood of the singularity.

IV. Series Treatment at Reentrant Corners

In a paper published some 20 years ago, Motz[9] discussed the boundary singularity problem in connection with the solution of potential problems by relaxation methods. We have followed Motz's earlier work and used a series expansion in circular harmonics to describe the field in the neighborhood of a reentrant corner. This treatment is applicable to any wedge shaped reentrant corner including a knife-edged boundary. Consider the infinite conducting wedge shown in Fig. 4, where the potential $\phi=\phi_0$ on the boundary surface. Using a polar coordinate system (r, θ), the wedge surfaces are defined by $\theta=0$, $\theta=\theta_0$, with the wedge vertex located at $r=0$. The designation $r=R$ simply represents a particular length (or interval) measured from the vertex ($r=0$) to a point on the wedge surface. In the region exterior to the wedge ($r\geq 0$, $0\leq\theta\leq\theta_0$), the solution of Laplace's equation can be expressed as an infinite series of circular harmonics:

$$\phi(r,\theta) = \phi_0 + \sum_{n=1}^{\infty} a_n r^{(n\pi/\theta_0)} \sin\left(\frac{n\pi\theta}{\theta_0}\right). \qquad (13)$$

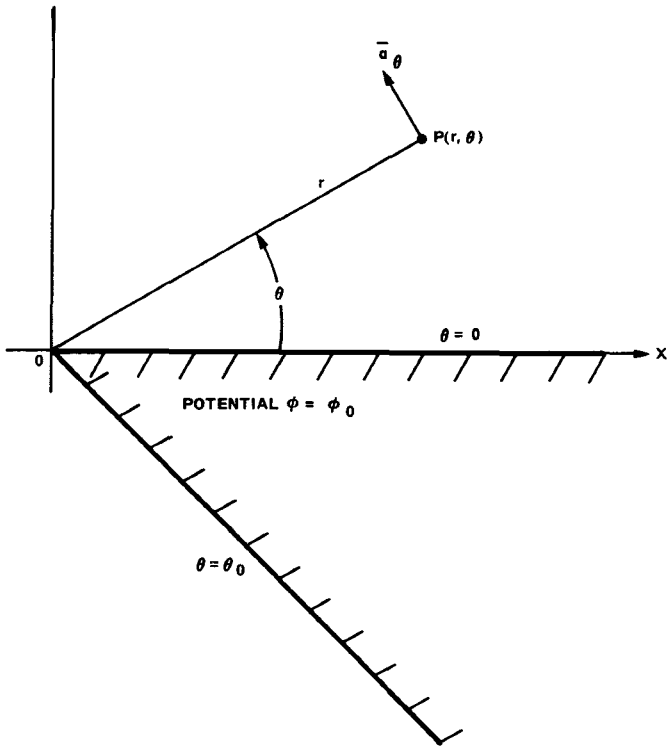

Fig. 4. Infinite conducting wedge.

The electric field intensity normal to the wedge surface is given by

$$\bar{E} = \bar{a}_\theta\left(-\frac{1}{r}\frac{\partial\phi}{\partial\theta}\right)$$

$$= -\bar{a}_\theta \sum_{n=1}^{\infty} a_n\left(\frac{n\pi}{\theta_0}\right) r^{((n\pi/\theta_0)-1)} \cos\left(\frac{n\pi\theta}{\theta_0}\right) \qquad (14)$$

where $\bar{a}_\theta$ is a unit vector in the θ direction, and $\theta=0$ or $\theta=\theta_0$ in (14). In applying (14) to the right-angle reentrant corner ($\theta_0=3\pi/2$), we elected to use four terms of (14) to represent the normal electric field. Thus, at the surfaces $\theta=0$ and $\theta=\theta_0=3\pi/2$, (14) yields

$$\bar{E}(r, 0) = \bar{y}[c_1 r^{-1/3} + c_2 r^{1/3} + c_3 r + c_4 r^{5/3}],$$

$$\bar{E}\left(r, \frac{3\pi}{2}\right) = -\bar{x}[c_1 r^{-1/3} - c_2 r^{1/3} + c_3 r - c_4 r^{5/3}] \qquad (15)$$

where $\bar{x}$ and $\bar{y}$ are unit vectors. The coefficients of series of the type (13) or (14) can be related to the finite-difference solution in a variety of ways. The determination of the "best" way is a study in itself. In the case of the right-angle corner, the coefficients of (15) were determined by equating (15) to the finite-difference value of $|\partial\phi/\partial n|$ at the locations $r=R$ and $r=2R$ on the surfaces $\theta=0$ and $\theta=3\pi/2$. This elementary method of determining the series coefficients was the only one that was used and other methods were not investigated. When a symmetrical bend ($g=b$) is treated using (15), $c_2=c_4=0$ and (15) reduces to a two term series because the potential gradient is symmetrical about the corner.

The surface charge per unit area on a conducting surface is given by $\rho_s = \epsilon E_n$, where ϵ is the permittivity of the medium and E_n is the electric field normal to the surface. As (15) shows, the surface charge becomes infinite as $r^{-1/3}$ as $r \rightarrow 0$ at a 90 degree corner. The series (15) can be integrated term by term to obtain a closed form expression for the charge per unit length over the interval from $r=R$ to the corner. Let $q(R)$ denote the charge per unit length over $0 \leq r \leq R$, hence

$$q(R) = \epsilon \int_0^R \bar{E} \cdot \bar{n} dr = -\epsilon \int_0^R \left(\frac{\partial \phi}{\partial n}\right) dr. \qquad (16)$$

It follows from (15) and (16) that

$$q(R)\Big|_{\theta=0} = \epsilon \frac{3}{2} R^{2/3} \left[c_1 + \frac{c_2}{2} R^{2/3} + \frac{c_3}{3} R^{4/3} + \frac{c_4}{4} R^2 \right],$$

$$q(R)\Big|_{\theta=3\pi/2} = \epsilon \frac{3}{2} R^{2/3} \left[c_1 - \frac{c_2}{2} R^{2/3} + \frac{c_3}{3} R^{4/3} - \frac{c_4}{4} R^2 \right]. \qquad (17)$$

The assumptions and approximations leading to (17) are evident. The accuracy that can be achieved using (17) will be a function of the mesh size h and the interval R. Referring to Fig. 2(a), (17) was used to calculate the charge per unit length about corner C' and the result was compared to the exact solution obtained from conformal mapping. The results are presented in Fig. 5 which shows the percent error in $q(R)$ as a function of the normalized interval R/h. Fig. 5 indicates that the minimum error in the representation (17) may occur when R is approximately equal to $b/4$ and that an error of less than 0.5 percent is quite feasible using (17).

Suppose that (17) is applied to an asymmetrical bend where g is considerably different from b. As a result of Fig. 5, we should expect the accuracy of $q(R)$ to be considerably different on the surfaces $\theta=0$ and $\theta=3\pi/2$ because the normalized intervals R/b and R/g are different. Surprisingly, this is not the case, as is indicated in Fig. 6 which shows the percent error in $q(R)$ for a bend where $g=4b$. q_1 and q_2 denote the charge on the horizontal and vertical surfaces, respectively. Results obtained using both the five- and nine-point operators are given in the figure. In contrast to Fig. 5, when the interval $R/h=4$ which corresponds to $R=b/2$ and $R=g/8$, we see that the error in $q_1(R)$ *and* $q_2(R)$ is less than 0.1 percent provided that the five-point operator is used.

The series treatment described above was used to determine the total charge on the inner conductor of a square coaxial transmission line. Because of symmetry, only one quadrant of the cross section shown in Fig. 7 was treated by the finite-difference method. The exact solution of this configuration is available from conformal mapping.[19] For the geometry where $AB=2(CD)$, the capacitance per unit length of the line is $C=(10.234)\epsilon$, where ϵ is the permittivity in farads per meter. Using a mesh division of $b/h=40$ yielded 4719 interior nodes. Setting the residual test constant $m=10^{-6}$, the resulting machine time was 58 seconds. The formulation (17) was used to calculate the charge over the interval $0 \leq r \leq R$, while the charge from $r=R$ to the midpoint of the boundary was calculated by numerical integration of the normal derivatives. The results are given in Fig. 7 which shows the percent error in C/ϵ as a function of the interval R/b over which the series treatment is applied. Notice that the error was 1.85 percent for $R/b=0$, that is, when the charge was determined by numerical integration over the entire inner boundary surface. The error was reduced to 0.06 percent by means of the series treatment when the interval $0.25 \leq R/b \leq 0.30$ was used in the application of (17).

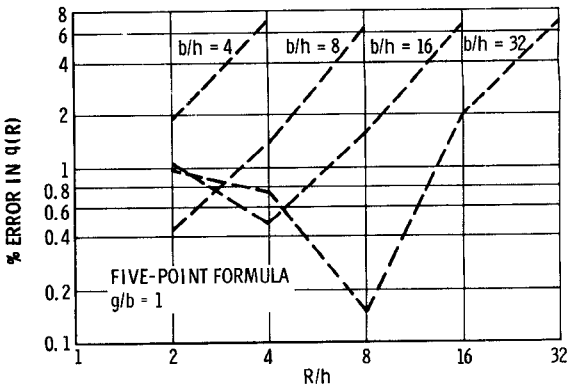

Fig. 5. Percent error in the integrated charge at a 90 degree corner ($g=b$).

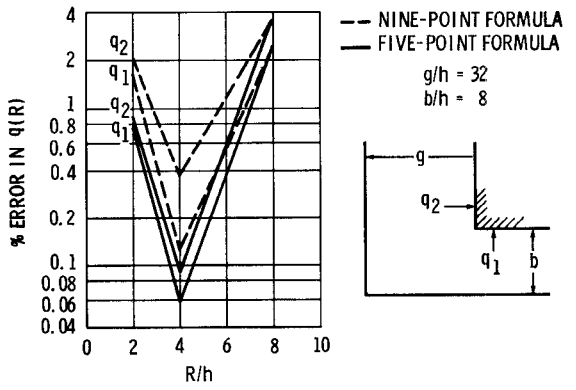

Fig. 6. Percent error in the integrated charge at a 90 degree corner ($g=4b$).

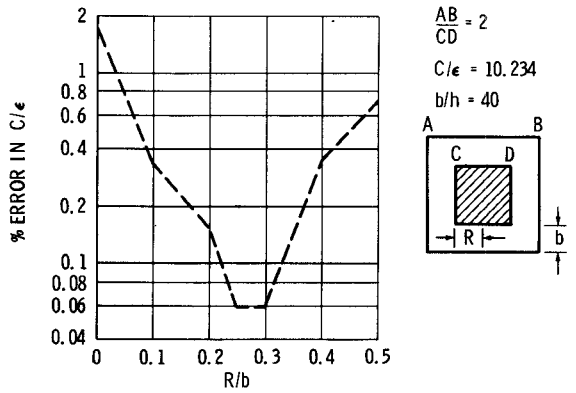

Fig. 7. Percent error in C/ϵ for the square coaxial transmission line.

V. Conclusions

In the preceding work we have investigated, in some detail, the problem of accuracy in the numerical finite-difference solution of Laplace's equation. Admittedly, the investigation was specialized to the calculation of normal derivatives on boundary surfaces near field singularities. The effect of the mesh size and the lattice point residuals on the solution is well established but some question remains concerning the difference operator. In the situation considered here, where normal derivatives are evaluated on boundaries near a singularity, it would appear that the five-point operator is the better choice. However, in the case of a well behaved boundary value problem without boundary singularities, we would expect the nine-point operator to yield the more accurate results.

It has been shown that a finite series of circular harmonics can provide a very accurate representation of the surface charge on a wedge shaped boundary, and that the integral of the charge can be accurately determined. It follows from Gauss's law that the characteristic impedance or capacitance per unit length of a TEM line can be determined by integrating $\epsilon(-\nabla\phi\cdot\hat{n})$ over an arbitrary contour that encloses one of the conductors. As a result, it is common practice in mesh problems to select a contour which is removed from edges or corners so as to avoid the errors introduced by the boundary singularities. In order to calculate the attenuation constant of the line, however, one *must* integrate the normal field over the conductor boundaries. In such cases, one must utilize some refinement such as the harmonic series treatment in order to obtain accurate results with the finite-difference method.

Acknowledgment

The author wishes to acknowledge that the extensive computer programming associated with this study was performed by S. P. Jue of the Mathematical Analysis Section, Hughes Aircraft Company.

References

[1] H. E. Green, "The numerical solution of some important transmission-line problems," *IEEE Trans. Microwave Theory and Techniques*, vol. MTT-13, pp. 676–692, September 1965.

[2] M. V. Schneider, "Computation of impedance and attenuation of TEM-lines by finite difference methods," *IEEE Trans. Microwave Theory and Techniques*, vol. MTT-13, pp. 793–800, November 1965.

[3] M. E. Armstrong, R. H. DuHamel, J. W. Duncan, and H. A. Uyeda, "Design and development of a tapered-line magic-*T*," Hughes Aircraft Co., Fullerton, Calif., Final Engrg. Rept., FR 65-14-133, July 1965.

[4] W. J. Getsinger, "Fringing capacitances for offset coupled strips in shielded strip line," M.I.T. Lincoln Lab., Lexington, Mass., Tech. Note 1965-33, Defense Doc. Center, AD 618 927, July 1965.

[5] J. P. Shelton, Jr., "Impedances of offset parallel-coupled strip transmission lines," *IEEE Trans. Microwave Theory and Techniques*, vol. MTT-14, pp. 7–15, January 1966.

[6] C. T. Carson and G. K. Cambrell, "Upper and lower bounds on the characteristic impedance of TEM mode transmission lines," *IEEE Trans. Microwave Theory and Techniques* (*Correspondence*), vol. MTT-14, pp. 497–498, October 1966.

[7] G. E. Forsythe and W. R. Wasow, *Finite-Difference Methods for Partial Differential Equations*. New York: Wiley, 1960, sec. 23, pp. 283–329.

[8] ——, *op. cit.*, p. 311.

[9] H. Motz, "The treatment of singularities of partial differential equations by relaxation methods," *Quart. Appl. Math.*, vol. 4, pp. 371–377, 1947.

[10] R. E. Collin, *Field Theory of Guided Waves*. New York: McGraw-Hill, 1960, pp. 119–169.

[11] L. V. Kantorovich and V. I. Krylov, *Approximate Methods of Higher Analysis*. Groningen, The Netherlands: Noordhoff, 1958, pp. 179–185.

[12] D. Young, "Iterative methods for solving partial difference equations of elliptic type," *Trans. Am. Math. Soc.*, vol. 76, pp. 92–111, January 1954.

[13] S. P. Frankel, "Convergence rates of iterative treatments of partial differential equations," *Math. Tables and Other Aids to Computation*, vol. 4, pp. 65–75, April 1950.

[14] B. A. Carré, "The determination of the optimum accelerating factor for successive over-relaxation," *Computer J.*, vol. 4, pp. 73–78, 1961.

[15] W. E. Milne, *Numerical Solution of Differential Equations*. New York: Wiley, 1953, p. 217.

[16] E. Weber, *Electromagnetic Fields*. New York: Wiley, 1950, pp. 325–362.

[17] W. G. Bickley, "Formulae for numerical differentiation," *Math. Gazette*, vol. 25, pp. 19–27, 1941.

[18] L. F. Richardson and J. A. Gaunt, "The deferred approach to the limit," *Phil. Trans. Roy. Soc. London*, ser. A, vol. 226, pp. 229–361, 1927.

[19] F. Bowman, *Introduction to Elliptic Functions*. New York: Wiley, 1953, pp. 99–104.